

REPORT DOCUMENTATION PAGE				Form Approved OMB No. 0704-0188	
Public reporting burden for this collection of information is estimated to average 1 hour per response, including the time for reviewing instructions, searching existing data sources, gathering and maintaining the data needed, and completing and reviewing this collection of information. Send comments regarding this burden estimate or any other aspect of this collection of information, including suggestions for reducing this burden to Department of Defense, Washington Headquarters Services, Directorate for Information Operations and Reports (0704-0188), 1215 Jefferson Davis Highway, Suite 1204, Arlington, VA 22202-4302. Respondents should be aware that notwithstanding any other provision of law, no person shall be subject to any penalty for failing to comply with a collection of information if it does not display a currently valid OMB control number. PLEASE DO NOT RETURN YOUR FORM TO THE ABOVE ADDRESS.					
1. REPORT DATE (DD-MM-YYYY) 10-06-2008		2. REPORT TYPE Technical Paper		3. DATES COVERED (From - To)	
4. TITLE AND SUBTITLE Effect of a Phase Angle on Coaxial Jet Behavior Spanning Sub- to Supercritical Pressures (Preprint)				5a. CONTRACT NUMBER	
				5b. GRANT NUMBER	
				5c. PROGRAM ELEMENT NUMBER	
6. AUTHOR(S) Ivett A. Leyva, Juan Rodriguez, & Douglas Talley (AFRL/RZSA); Bruce Chehroudi (ERC)				5d. PROJECT NUMBER	
				5e. TASK NUMBER 23080533	
				5f. WORK UNIT NUMBER	
7. PERFORMING ORGANIZATION NAME(S) AND ADDRESS(ES) Air Force Research Laboratory (AFMC) AFRL/RZSA 10 E. Saturn Blvd. Edwards AFB CA 93524-7680				8. PERFORMING ORGANIZATION REPORT NUMBER AFRL-RZ-ED-TP-2008-211	
9. SPONSORING / MONITORING AGENCY NAME(S) AND ADDRESS(ES) Air Force Research Laboratory (AFMC) AFRL/RZS 5 Pollux Drive Edwards AFB CA 93524-7048				10. SPONSOR/MONITOR'S ACRONYM(S)	
				11. SPONSOR/MONITOR'S NUMBER(S) AFRL-RZ-ED-TP-2008-211	
12. DISTRIBUTION / AVAILABILITY STATEMENT Approved for public release; distribution unlimited (PA #08222A).					
13. SUPPLEMENTARY NOTES Submitted for presentation at the ILASS-Europe Meeting, to be held in Lake Como, Italy, 8-10 Sep 2008.					
14. ABSTRACT This paper describes the effects of phase angle of an acoustic pressure field on a shear coaxial jet. The jet is forced with a transverse acoustic field, made up of two acoustics sources with p'_{RMS}/p_{mean} up to 3.1%. The chamber pressure ranges from 1.5 to 5.0 MPa. The momentum flux ratio (MR) between the outer and inner jet varies from 0.02 to 23 and the velocity ratio from 0.25 to 23. The shear coaxial geometry is selected because of its application to liquid rocket engines. The jet was analyzed by taking high speed images and exit-plane temperature measurements. This work continues previous work where the jet was excited with one acoustic source; therefore the jet location was fixed with respect to the acoustic field. For nearcritical pressures, the cases with $MR < 1$ and $MR > 9$ were least sensitive to the acoustic field and phase angles. For the cases, $MR = 1.1$ to 4.9 the trends of L/D qualitatively followed the p' field trends. The maximum L/D was found around the maximum value of p' and viceversa. For these data, it seems like the dark core length is more affected, in terms of its reduction, by high acoustic velocity amplitude and not high pressure amplitudes.					
15. SUBJECT TERMS					
16. SECURITY CLASSIFICATION OF:			17. LIMITATION OF ABSTRACT SAR	18. NUMBER OF PAGES 9	19a. NAME OF RESPONSIBLE PERSON Dr. Douglas Talley
a. REPORT Unclassified	b. ABSTRACT Unclassified	c. THIS PAGE Unclassified			19b. TELEPHONE NUMBER (include area code) N/A

EFFECT OF PHASE ANGLE ON COAXIAL JET BEHAVIOR SPANNING SUB- TO SUPERCRITICAL PRESSURES (Preprint)

Ivett A Leyva*, Juan Rodriguez°, Bruce Chehroudi⁺, Douglas Talley*

*AFRL/RZSA Edwards AFB, Ca,
°Graduate Student, UCLA, Los Angeles, Ca
+ ERC, Edwards AFB, Ca

ABSTRACT

This paper describes the effects of phase angle of an acoustic pressure field on a shear coaxial jet. The jet is forced with a transverse acoustic field, made up of two acoustics sources with $p'_{\text{RMS}}/p_{\text{mean}}$ up to 3.1%. The chamber pressure ranges from 1.5 to 5.0 MPa. The momentum flux ratio (MR) between the outer and inner jet varies from 0.02 to 23 and the velocity ratio from 0.25 to 23. The shear coaxial geometry is selected because of its application to liquid rocket engines. The jet was analyzed by taking high speed images and exit-plane temperature measurements. This work continues previous work where the jet was excited with one acoustic source; therefore the jet location was fixed with respect to the acoustic field. For nearcritical pressures, the cases with $MR < 1$ and $MR > 9$ were least sensitive to the acoustic field and phase angles. For the cases, $MR = 1.1$ to 4.9 the trends of L/D qualitatively followed the p' field trends. The maximum L/D was found around the maximum value of p' and viceversa. For these data, it seems like the dark core length is more affected, in terms of its reduction, by high acoustic velocity amplitude and not high pressure amplitudes.

INTRODUCTION

The motivation for this work springs from the problem of combustion instabilities in liquid rocket engines. One of the unit physics problems that can be defined to try to understand the larger problem of combustion instabilities is the problem of the interaction of an acoustic field with a typical rocket injector. We choose to study the effects of a transverse acoustic field vs. a longitudinal field, because the former interactions are some of the most destructive to a rocket engine. Also, we choose to first investigate a shear coaxial injector because they are widely used in liquid rocket engines (LRE's). A key advantage of coaxial jets is that as the Momentum Flux Ratio (MR) between the outer jet and the inner jet increases mixing between the two jets increases so that uniformity can be obtained in relatively short distances from the exit plane. The Space Shuttle Main Engine (SSME) and the Vulcan engine for the Ariane 5 are examples of LRE's designed to operate above the critical pressures of each propellant individually. Hence, in our studies, we vary the chamber pressure from sub to supercritical values. In a typical application of a coaxial injector for a LOX/LH2 engine (e.g SSME), the oxygen is injected at subcritical temperatures in the center jet while the hydrogen is injected at supercritical temperatures, after being used as a coolant for the engine nozzle, in the coaxial jet. For these flows, the mixture no longer has a singular critical point but rather there are critical mixing lines that define its thermodynamic state [1]. Because of the added complexity introduced when working with mixtures, N_2 is used as the sole working fluid in this study. A typical operating velocity ratio (VR) between the outer and inner jets is about 10 arrived at from empirical evidence that injectors operating at these high

VR's were more stable against combustion instabilities [2,3]. Therefore in our studies we vary the VR and MR from less than 1 to the low 20's for both variables.

This paper is focused specifically on the effects of the phase of the acoustic pressure and velocity field on the coaxial jet flow. In previous experiments performed in the same lab there was one acoustic source at one end of the test chamber and a non-movable reflective wall at the other end. This meant that the relation of the position of the jet with respect to the acoustic wave profile was fixed. By adding a second identical resonator the magnitude and relative position of the pressure and velocity acoustic field with respect to the jet are now varied. Preliminary results for a few run conditions were presented before in the papers by Leyva et. al. [4] and Rodriguez et. al. [5]. This paper presents a complete set of data for one geometry. The data includes three chamber pressures and several MR's for each pressure. The axial length of the dark core is the main metric studied in this paper. An analysis of the spreading angle of the inner and outer jet under an acoustic field will be the next metric to be analyzed in a future paper.

EXPERIMENTAL SETUP

The experiments detailed here were performed at the Cryogenic Supercritical Laboratory (EC-4) at the Air Force Research Laboratory (AFRL) at Edwards Air Force Base, CA Figure 1 shows the main chamber and the supporting systems. In the current setup, ambient temperature N_2 is used to supply the inner and outer jet and also to pressurize the chamber. As a note, the critical temperature of N_2 is 126.2 K and its critical pressure is 3.39 MPa. . Both the inner and the

outer jets are cooled by heat exchangers (HE's) using liquid nitrogen obtained from a cryogenic tank. One heat exchanger cools the inner jet and other two cool the outer jet. Depending on the setup, one of these HE's can be bypassed to modify the cooling patterns. The mass flow rates of liquid nitrogen through the HE's are regulated in order to control the temperature of the jets. These rates are measured with Porter® mass flow meters (122 and 123-DKASVDAA) at ambient conditions to avoid difficulties with mass flow rate measurement at cryogenic temperatures. An inner chamber was built and housed inside the main chamber to maintain the amplitude of the acoustic oscillations to a maximum at the test section. The inner chamber is 6.6 cm high, 7.6 cm wide and 1.3 cm deep (see Fig. 1).

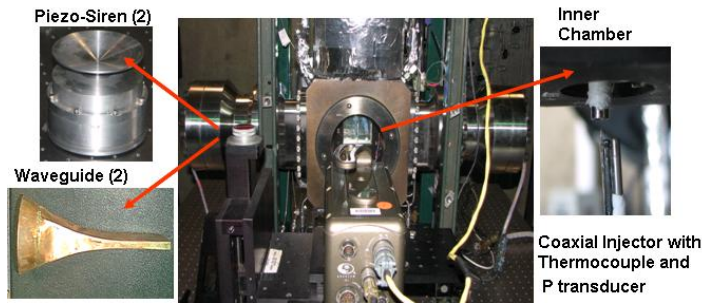


Figure 1. Experimental Setup

The inner tube making the inner jet has an inner diameter, $D1$, of 0.51 mm with length-to-diameter ratio of 100. The inner jet exit plane is recessed by 0.3 mm from the outer jet. The outer annular jet's inner diameter, $D2$, is 1.59 mm with outer diameter, $D3$, of 2.42 mm. For the outer jet, the length-to-mean-width of the annular passage is 67. The coaxial injector is shown in Fig. 2.

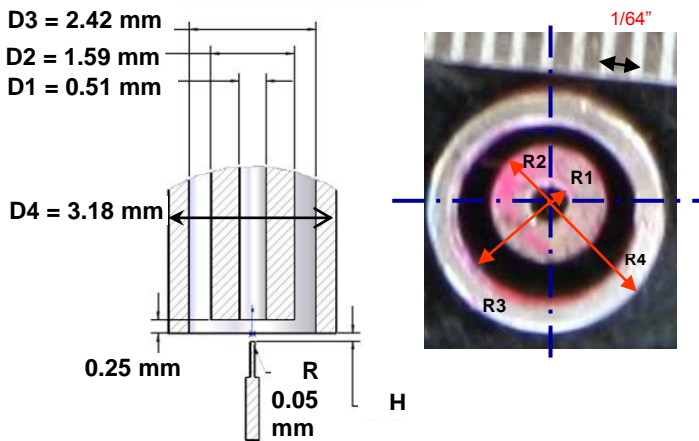


Figure 2. Details on the geometry of the shear coaxial injector used in this study.

The chamber pressure is measured with a Stellar 1500 transducer. An unshielded type E thermocouple with a bead diameter of 0.1 mm is used to measure the temperature of the jets. The accuracy of this thermo-couple was checked with an RTD and found to be ± 1 K. Also, a Kulite® XQC-062 pressure transducer is used to measure the pressure near the location of the thermocouple tip at a sampling frequency of 20 kHz (see bottom right picture in Fig. 1). Both the pressure transducer and the thermocouple are moved in the plane perpendicular to the jet axis with two linear positioning stages built by Attocube Systems AG. Each stage has a range of about 3 mm in 1 dimension with step sizes in the order of

0.01 mm. One stage was placed on top of the other with their axis of movement perpendicular to each other for a total maximum interrogation area of 3 mm by 3 mm. The thermocouple and pressure transducer were fixed to a custom made probe stand mounted on top of the positioning assembly. In turn, the linear stages were placed at the top end of a shaft that rested on a large 4-inch range linear stage built by SETCO™ outside the main chamber. Thus, the temperature probe approaches the coaxial jet from the bottom and it can get arbitrarily close to the exit plane. This thermocouple has even been used to measure the temperature within the recess of the inner jet.

The density, viscosity, and surface tension from the measured flow rates, chamber pressure and jet temperature are obtained using NIST's REFPROP® online database [6,7]. From these properties, Re , We , outer to inner jet velocity ratio (VR) and MR for a given condition are then calculated.

The coaxial flow was visualized using a Phantom® 7.1 CMOS camera. The camera can be seen facing the main chamber in the bottom left picture of Figure 1. Backlit images with a resolution from 128x224 to 196x400 pixels were obtained, with each pixel representing an area of approximately 0.08 mm by 0.08 mm. The framing rate was 20-25 kHz. The number of images saved per run was 1000 on average. The jet was backlit using a Newport® variable power arc lamp set at 160 W. The dark core lengths are measured from 998 images using a MATLAB® subroutine based on the Otsu technique [8] to find a grayscale threshold which helps distinguish the inner core from the rest of the image (see Fig. 3).

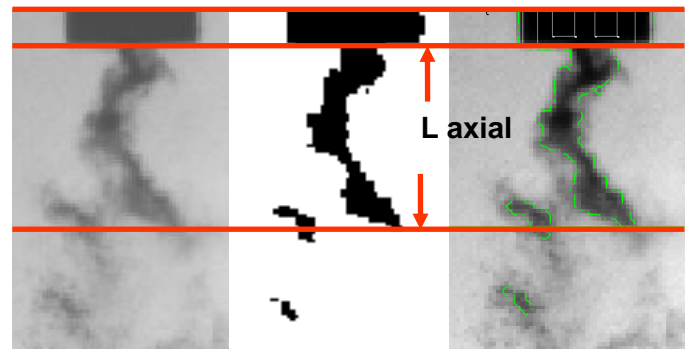


Figure 3. Definition of Axial Dark Core Length, L_{axial} . Leftmost image is a typical image. The middle image shows the original image after it has been thresholded to a binary image. The right image shows the contour from which the axial length is calculated.

The two piezo-sirens used to generate the transverse acoustic field were custom-designed by Hersh Acoustical Engineering, Inc. (see Fig. 1). The principle by which the piezo-sirens work as acoustic drivers is relatively simple. A sinusoidal voltage signal moves a piezo element with an aluminum cone attached to it, which in turn produces acoustics waves. When the two drivers have a zero degree phase angle difference then the movement of the piezo-siren cones is synchronized and they move in opposite directions. On the contrary, when the two drivers have a 180-degree phase difference the cones move in the same direction, or they 'chase' each other. This behavior is represented by the sketches in Fig. 4. A Fluke® signal generator was used to drive the piezo-sirens with a sinusoidal wave at a chosen driving frequency and phase angle between them. The fre-

quency was manually varied until the highest amplitudes of the pressure waves were obtained. These frequencies spanned a range between 2.93 and 3.09 kHz. Then the signals were amplified and fed to the piezo-sirens. The voltage supplied each driver was kept constant. A waveguide with a catenary contour was used to guide the waves from a circular cross-section at the end of the aluminum cone to the rectangular cross-section of the rectangular inner chamber.

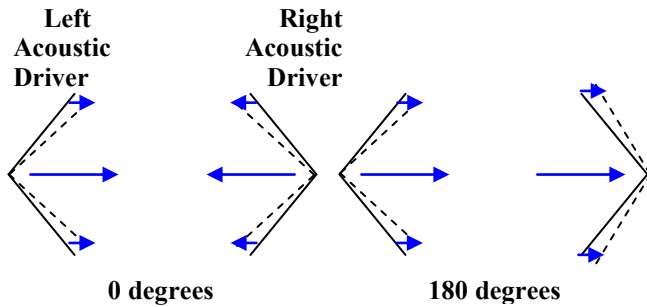


Figure 4. Simplified diagram of the two acoustic drivers at a 0° and 180° phase angle.

RESULTS

A series of runs were made at three nominal chamber pressures to span sub to supercritical chamber pressures. The detailed list of run conditions is shown in Table 1 in the appendix. For each chamber pressure several MR's were taken and for each MR the two acoustic sources were run at phase angles from 0 to 360 deg at intervals of 45 degrees. A qualitative sample of how the jet behaves for the different phase angles is first shown in Fig. 5. Here the first figure shows the jet with no acoustics. In this case, the pressure is subcritical and the inner jet is a liquid within 1 or 2 degrees K of the saturation temperature, and the outer jet is a gas. We can see that the dark core, or inner jet, is longest for the case with no acoustics, or baseline. Immediately when the acoustic field is turned on (0 deg), the jet is affected by the acoustics and the inner core is bent and shortened. We can also see how the outer jet is bent compared to the baseline case but not as dramatically. The bending and shortening of the dark core continues as the phase angle is increased and the minimum dark core length and most bending (qualitatively measured by the horizontal extend of the inner jet travel) are achieved at around 135-180 deg where we expect to have the highest amplitude of the velocity field.

The results on the shortening of the dark core length for all the cases run are compiled in Fig. 6. In this case, the y axis is the axial dark core length non-dimensionalized by the inner diameter of the inner jet, D_1 . The x-axis represents the phase angle between the two acoustic sources. As a convention, the angle is only changed on the right source with respect to the left source (Fig.1). The leftmost point in every graph corresponds to the case where no acoustics were on. In previous papers [9-10] it was shown that as the MR increases the axial dark core length decreases regardless of the chamber pressure. However, the behavior of the dark core length falls in two branches, one for subcritical pressure in which $L \sim A/MR^{0.2}$ and the other for near and supercritical pressures where $L \sim B/MR^{0.5}$. The results

obtained here for the case of no-acoustics agree with those previous results. Overall, we observe that for the chamber pressures studied here, as MR increases the axial length decreases for all phase angles. For $MR > \sim 9$, L/D_1 is $< \sim 7$ for the three chamber pressures and phase angles presented here. Also, the absolute (as compared to percentage) variation of the core length with respect to the baseline case as a function of phase angle decreases with MR. In other words, for the cases with the higher MR's the curves become more and more flat. For MR around 1-3 the curves of L/D_1 show some curvature. For the specific case of subcritical pressures, we observe a grouping in the data. For the case of $MR < 1$ the lengths are longest as mentioned previously. However, for the three cases of $MR=1$ to $MR=4.2$, we see very good agreement among these cases. The L/D values cluster around 9 to 13 and they have about the same shape. Their minimum occurs around 180 deg and their maximum around 315-360 degrees. This is consistent with previous observations that the jet is more affected by high velocity fields than by high pressure fields. Finally, for the cases with $MR > 9$, the data becomes less sensitive to phase angle. For the case of nearcritical pressures, there is a similar grouping on the data, with the two curves for $MR=0.55$ and 1 being longest, then the three curves corresponding to $MR=1.1$ to 2.1 clustering around each other and showing the same curvature. In this case also, the minimum is around 180 deg and the maximum is around the ends of the curve. Note that while the case for $MR=2.9$ follows the same curvature as these three cases, because the values for L/D are lower, it cluster more with the high MR curves. A similar grouping can be observed for the case of supercritical pressure. However for the case of supercritical pressure, the curves for $MR=2.4$ to 9.9 cluster together with low L/D 's. For the case of near and supercritical pressures the dark core length varies by an order of magnitude between the lowest and highest MR's run.

Another way to look at the effect of the phase angle on the dark core length is to look at the ratio of the new dark core with acoustics to the baseline value with no acoustics. The results are shown in Fig. 7. The data is the same as in the previous figure but for each MR, the dark core lengths with acoustics are normalized by the respective baseline value. This is done to see if as the dark core length decreases with MR, its percentage decrease with acoustics also decreases. As it turns out, we see that for all the pressures, when the MR is larger than ~ 9 the change in length for all phase angles varies up to 20%. The biggest percentage reductions are for MR around 1 to 3. This is consistent with previous data reported in papers [9-10] where the maximum effect of a single acoustic source on the axial dark core length was found to be for $\sim 1 < MR < \sim 4$. Plotting the data in this way reveals that while the absolute variation of the dark core length for a given MR is usually greater for subcritical pressures, the percentage change for the MR's explored in this study is about the same for the three pressures studied. That is, the percentage change of the axial dark core length seems to be no greater than 50% for all cases. We also note that the case of supercritical pressures shows the most scatter on the data.

Since we are varying the phase of the acoustic field with respect to the exit of the jet, it is interesting to find out if the dark core length directly responds to the variations of the

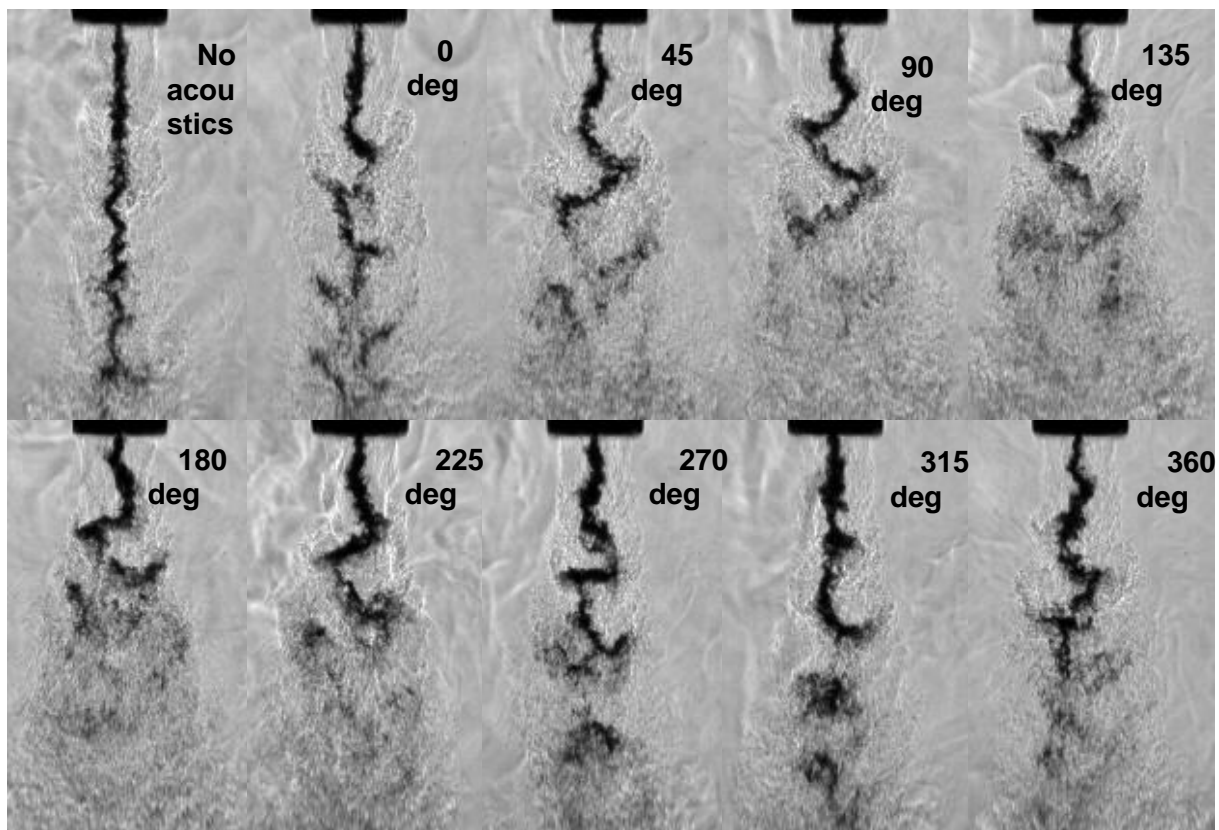


Figure 5. Images of a shear coaxial jet flow for different phase angles between two acoustic sources.

acoustic field. That is, as the acoustic pressure, p' , monotonically increases at the injector location, does the dark core length also monotonically increase or decrease? To answer this question, let's look in detail to a sample of superimposed traces of the acoustic field and the dark core length. We will look in detail to the nearcritical case. The results are shown in Figure 8. In general, the change on the location of the minimum in the p' field is due in part to the different frequencies that drove the acoustic sources. The frequency was chosen to give the max amplitudes in both drivers. The maximum p' amplitudes varied within 0.2 psi for all the cases examined here for the nearcritical pressures.

For the first case, $MR=0.56$, $VR=2.0$ and we can see that even though when the acoustics are turned on the dark core length decrease is statistically significant, the dark core length remains about constant for all the phase angles, except for the last point at 360 deg. This is not surprising since we have seen before that coaxial jets with $MR<1$ do not seem very sensitive to pressure fluctuations. Therefore, qualitatively, the trend of L/D does not follow the trend of p' , which has a minimum at around 135 deg. The inaccuracy of the acoustic pressure are not shown but it is ± 6.9 kPa according to the manufacturer. Therefore, the pressure variations fall within the accuracy of the transducer and the trends although mostly qualitative, agree very well with intuition where we would expect a minimum in acoustic pressure around 180 degrees.

The second case to consider has $MR=1.6$, $VR=2.8$. In this case, the qualitative trends of L/D and p' follow each other. Within the error bars we have a maximum L/D at the same phase angle where we have a maximum in the p' field. This would mean that when the pressure disturbance is maximum, the jet gets disturbed the least. Similarly the minimum L/D happens close to the minimum p' . This also points to the observation that it is the velocity fluctuations that most affect the jet. That is, when u' is highest, hence p' is lowest, the jet gets most decreased and bent. Notice also that p' for 0 deg and 360 deg are very close to each other, as they should be since this represents a full cycle returning to the same point

The following chart in Fig. 8 is for $MR=2.9$ $VR=4.1$. This and the previous chart ($MR=1.6$) are within the range of MR 's where we have previously seen the most effect on the dark core length. In this case, there is not a clear max or min for L/D but the range of max L/D is clustered around the max p' and the range of min L/D is clustered around the min p' . The last chart is for $MR=9.3$ $VR=5.5$. For this high MR , the dark core length has decreased significantly from the other cases. And once again, as it was the case for the low MR , the curve of L/D appears more flat. There does not seem to be a relation between the p' field and L/D . This is consistent with previous observations that for similar p' , for high MR 's the coaxial jet is not as disturbed as for $\sim 1 < MR < \sim 4$.

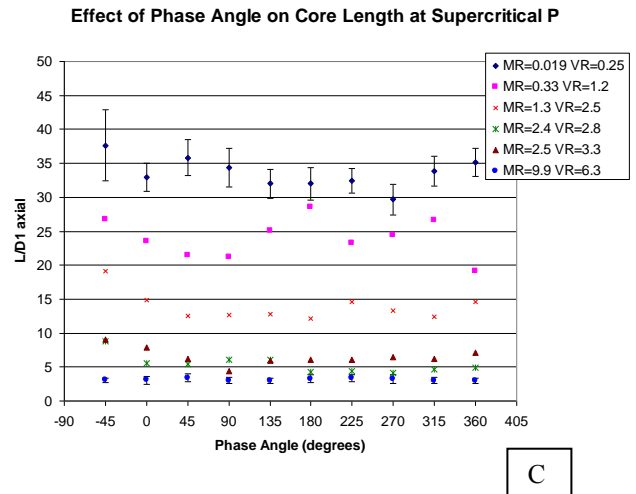
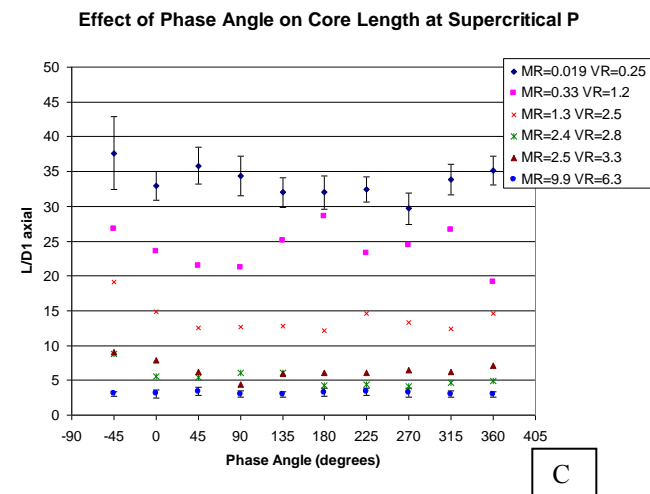
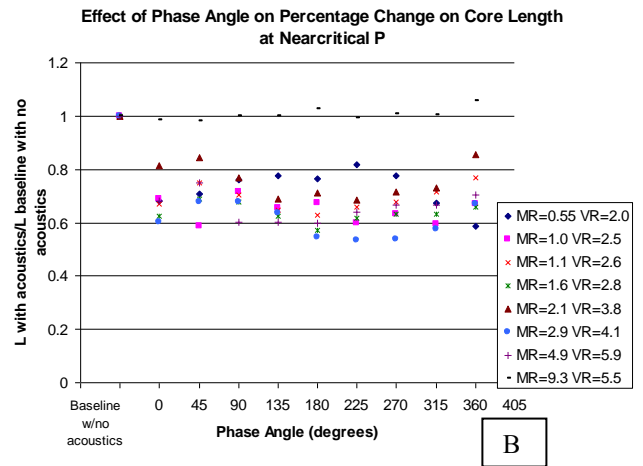
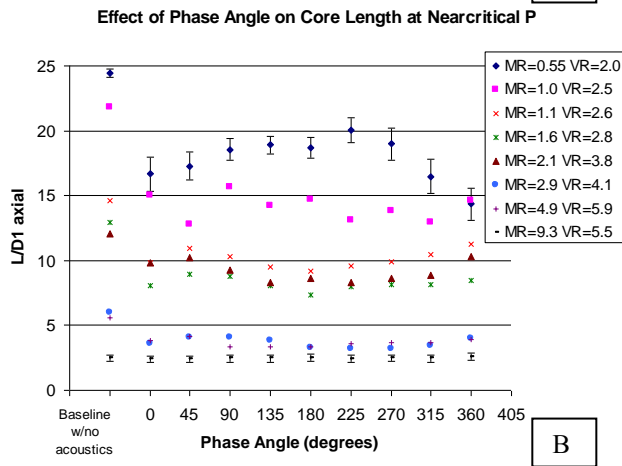
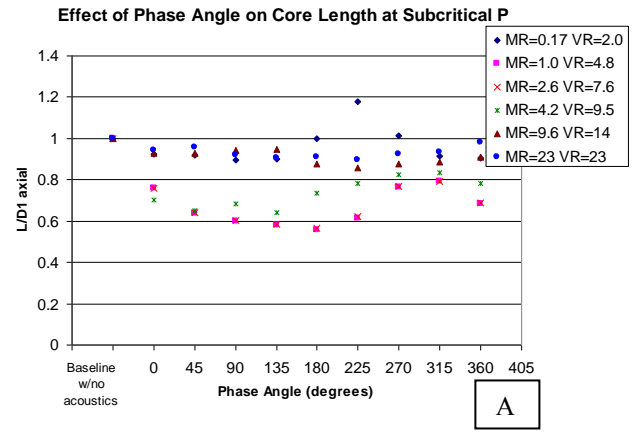
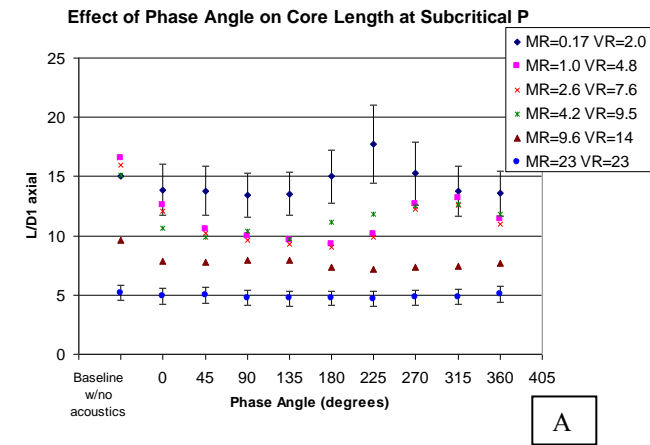


Figure 6. Effect of Phase Angle of the Axial Core Length for [A] Subcritical pressure, [B] Nearcritical pressure and [C] Supercritical pressure

Figure 7. Effect of Phase Angle of the percentage change of the Axial Core Length compared to the baseline case with no acoustics for [A] Subcritical pressure, [B] Nearcritical pressure and [C] Supercritical pressure

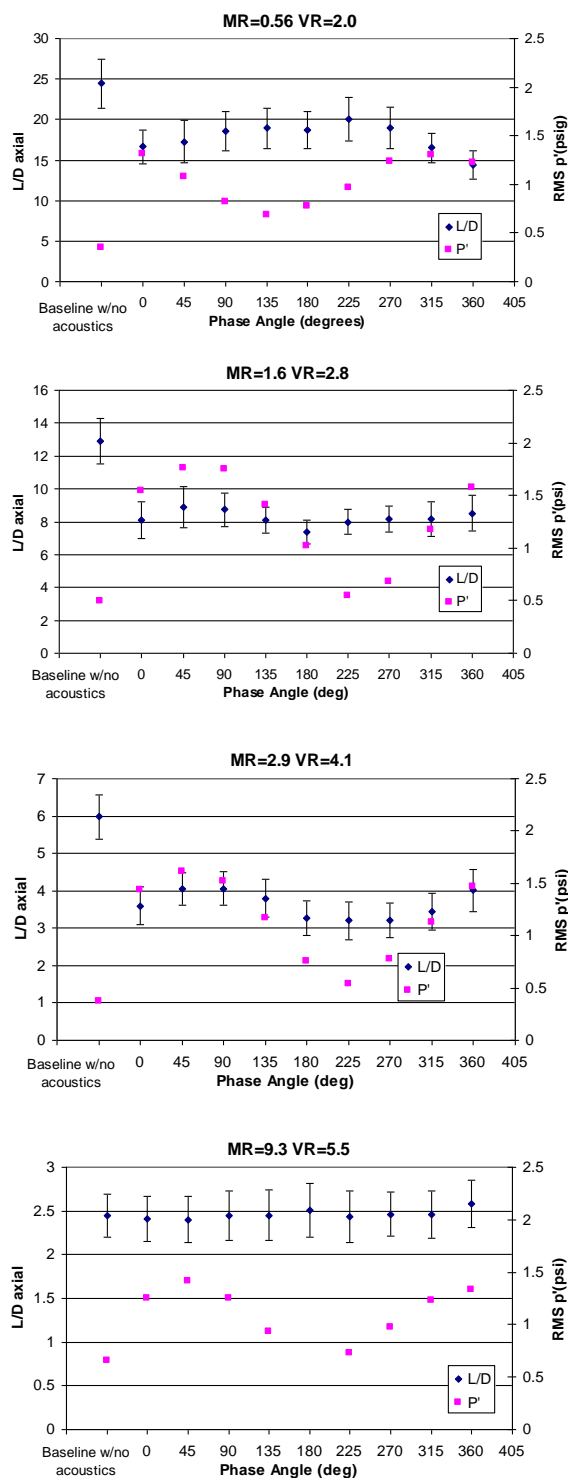


Figure 8. Comparison of acoustic pressure field and dark core length for the case of nearcritical pressures and different MR's

We have seen in the previous observations for the case of nearcritical pressures that the mixing mechanisms are different at different MR's. Once we set a relative momentum flux of the outer jet over the inner one, the interaction of the combined jets differs when it gets affected by a transverse acoustic source according to its MR. When

the MR is high (>9) the recirculation zone that gets set up in the region between the inner and the outer jet, due to the thick lip of the inner jet, becomes more prominent in the images and it starts to be of the same order of magnitude as the dark core itself. For these cases, when the jet is so short, the acoustics at any phase, move the jet back and forth but do not bend it. The contrary happens for low MR's (<1), where the jet is behaving more like a single jet. In these cases, the inner jet barely acquires curvature due to the acoustic field.

SUMMARY

In this paper we showed a complete set of data for a given geometry of a shear coaxial injector being perturbed by a transverse acoustic field. The acoustic field was set up by two acoustic sources. The phase angle of one acoustic source with respect to the other was changed from 0 deg to 360 deg. Three sets of operating chamber pressures spanning sub to supercritical values were chosen. For each chamber pressure an MR scan was done from $MR < 1$ to $MR > 9$. It was found that for the nearcritical pressure condition, the cases with $MR < 1$ and $MR > 9$ were least sensitive to the acoustic field. That is, the percentage variation of the dark core length for these cases was least. Also, the values of L/D were more insensitive to the phase angles. For the cases $MR = 1.1$ to 4.9 the trends of L/D qualitatively followed the p' field trends. That is, the maximum L/D was found around the maximum value of p' and vice versa. For these data, it seems like the dark core length is more affected, in terms of its reduction, by high acoustic velocity amplitude and not high acoustic pressure amplitudes.

NOMENCLATURE

Symbol	Quantity	SI Unit
D	Diameter	mm
P	Pressure	Pa
T	Temperature	T
\dot{m}	Mass flux	mg/s
p'	Acoustic pressure	Pa
ρ	Density	Kg/m ³
MR	Momentum flux ratio between outer and inner jet	Non dimensional
VR	Velocity ratio between outer and inner jet	Non dimensional

ACKNOWLEDGMENTS

The authors would like to thank Mr. Randy Harvey for his invaluable contributions in running and maintaining the facility and to Lt. Jeff Graham for his help with the data acquisition system and visualization technique. This work is sponsored by AFOSR under Mitat Birkan, program manager.

REFERENCES

1. Oschwald, M., Smith, J. J., Branam, R., Hussong, J., Schik, A., Chehroudi, B., Talley, D., "Injection of Fluids into Supercritical Environments", *Combustion Science and Technology*, Vol. 178, No. 1-3, 2006, pp. 49-100.
2. Oschwald, M., Smith, J. J., Branam, R., Hussong, J., Schik, A., Chehroudi, B., Talley, D., *Combustion Science and Technology* 1:49-100 (2006)
3. Hulka, J., Hutt, J. J., *Liquid Rocket Engine Combustion Instability*, AIAA Progress in Astronautics and Aeronautics, Yang, V., Anderson W. E., Eds., 1995, p. 40.
4. Leyva, I. A., Rodriguez, J. I., Chehroudi, B., Talley, D., "Preliminary Results on Coaxial Jets Spread Angles and the Effects of Variable Phase Transverse Acoustic Fields", AIAA-2008-0950
5. Rodriguez, J. I., Leyva, I. A., Chehroudi, B., Talley, D., Effects of a Variable-Phase Transverse Acoustic Field on a Coaxial Injector at Subcritical and Near-Critical Conditions", ILASS Americas, 21st Annual Conference on Liquid Atomization and Spray Systems, Orlando, Florida, May 18-21 2008
6. REFPROP, Reference Fluid Thermodynamic and Transport Properties, Software Package, Ver. 7.0, NIST, U.S. Department of Commerce, Gaithersburg, MD, 2002.
7. Thermophysical Properties of Fluid Systems (<http://webbook.nist.gov/chemistry/fluid>), NIST, U.S. Department of Commerce, Gaithersburg, MD, 2005
8. Otsu, N., *IEEE transactions on Systems, Man, and Cybernetics* 1:62-66 (1979).
9. Leyva, I. A., Chehroudi, B., Talley, D., "Dark-core analysis of Coaxial Injectors at Sub-, Near-, and Supercritical Conditions in a Transverse Acoustic Field", AIAA-2007-5456
10. Leyva, I. A., Chehroudi, B., Talley, D., "Dark-core analysis of Coaxial Injectors at Sub-, Near-, and Supercritical Conditions in a Transverse Acoustic Field", 54th JANNAF Meeting, Denver, CO, May 14-18, 2007.

APPENDIX

Table 1. Run Conditions

	T _{chamber} (K)	$\rho_{chamber}$ (kg/m ³)	P _{chamber} (MPa)	T _{outer} (K)	\dot{m}_{outer} (mg/s)	ρ_{outer_3} (kg/m ³)	u _{outer} (m/s)	T _{inner} (K)	\dot{m}_{inner} (mg/s)	ρ_{inner_3} (kg/m ³)	u _{inner} (m/s)	Freq. (kHz)	P' _{RMS max} (psi)	VR	MR
SUB															
sub1	233	22.0	1.50	191	310	22.0	4.3	109	279	630	2.2	2.98	3.12	2.0	0.17
sub2	231	22.2	1.50	183	790	28.8	11	109	283	630	2.2	3.06	2.91	4.8	1.0
sub3	226	21.9	1.45	183	1230	27.8	16.9	109	284	630	2.2	3.06	2.58	7.6	2.6
sub4	226	22.9	1.51	185	1560	28.7	20.9	109	279	630	2.2	2.96	2.27	9.5	4.2
sub5	210	24.9	1.50	182	2400	29.3	31.3	109	279	630	2.2	3.01	2.45	14	9.6
sub6	216	24.1	1.50	191	3640	27.7	50.3	109	279	630	2.2	3.02	2.36	23	23
NEAR															
near1	223	56.6	3.58	180	1060	75.4	5.38	123	290	520	2.8	3.08	1.31	2.0	0.55
near2	207	62.0	3.57	152	1570	101	5.95	117	289	590	2.4	3.04	1.56	2.5	1.0
near3	228	55.1	3.58	185	1590	72.4	8.40	126	293	440	3.3	3.00	1.71	2.6	1.1
near4	223	56.1	3.55	184	2170	72.3	11.5	127	294	360	4.0	3.01	1.65	2.8	1.6
near5	230	54.2	3.56	199	2120	65.1	12.5	126	292	440	3.3	3.03	1.76	3.8	2.1
near6	229	54.5	3.56	183	2690	73.1	14.1	126	292	420	3.4	3.05	1.61	4.1	2.9
near7	219	57.6	3.56	194	3080	67.4	17.5	125	289	480	3.0	3.06	1.71	5.9	4.9
near8	213	59.6	3.56	192	6460	68.3	36.2	128	295	220	6.6	2.93	1.41	5.5	9.3
SUPER															
super1	231	76.1	4.96	198	292	93.9	1.19	136	291	300	4.8	3.05	1.16	0.25	0.019
super2	231	76.1	4.96	193	997	97.7	3.90	130	292	460	3.1	3.01	1.48	1.2	0.33
super3	221	80.4	4.95	180	2050	109	7.19	128	291	490	2.9	3.01	1.55	2.5	1.3
super4	222	80.1	4.96	182	3110	107	11.1	134	288	360	3.9	3.05	1.47	2.8	2.4
super5	222	80.3	4.97	191	2820	99.5	10.8	131	293	440	3.3	3.09	1.81	3.3	2.5
super6	211	85.8	4.96	187	5820	103	21.6	132	286	410	3.4	3.05	1.55	6.3	9.9